Algorithm-Based Fault Tolerance for Spaceborne Computing: Basis and Implementations

Michael Turmon and Robert Granat
Machine Learning Systems Group, M/S 126-347
Jet Propulsion Laboratory
Pasadena, CA 91109
+1-818-393-5370
{turmon,granat}@aig.jpl.nasa.gov

Abstract —We describe and test the mathematical background for using checksum methods to validate results returned by a numerical subroutine operating in a fault- prone environment that causes unpredictable errors in data. We can treat subroutines whose results satisfy a necessary condition of a linear form; the checksum tests compliance with this necessary condition. These checksum schemes are called algorithm-based fault tolerance (ABFT). We discuss the theory and practice of setting numerical tolerances to separate errors caused by a fault from those inherent in finite-precision numerical calculations. Two series of tests are described. The first tests the general effectiveness of the linear ABFT schemes we propose, and the second verifies the correct behavior of our parallel implementation of them. We find that under simulated fault conditions, it is possible to choose a fault detection scheme that for average case matrices can detect 99% of faults with no false alarms, and that for a "worst-case" matrix population can detect 80% of faults with no false alarms.

Table of Contents

1. Introduction
2. General Considerations
3. Error Propagation: Theory
4. Error Propagation: Implementation
5. Results: Simulated Fault Conditions
6. Results: Fault-free parallel operation
7. Conclusions

0-7803-5846-5/00/$10.00 © 2000 IEEE

1. Introduction

Recently, there has been growing interest in transfering commercial high-performance computing technology into ultra-low power fault-tolerant architectures for space, with the aim of enabling new science investigation and discovery. Spaceborne science applications that intend to take advantage of this computing capability include the Next Generation Space Telescope (NGST), the Orbiting Thermal Imaging Spectrometer (OTIS), and the Solar Terrestrial Probe Project (STP). All of these applications require large amounts of computing capacity, as well as performance/power ratios that are at least an order of magnitude above those available in today's spacecraft.

However, as the processors to be used are current off-the-shelf components, they are not radiation-hardened, and will suffer from single event upsets (SEUs). The SEUs that occur require that the applications be self-checking, or tolerant of errors. It is in this context that we describe and test the mathematical background for using checksum methods to validate results returned by a numerical subroutine operating in an environment where SEUs can lead to unpredictable errors in data. We can treat subroutines that return results satisfying a necessary condition having a linear form; the checksum tests compliance with this necessary condition. These checksum schemes are called algorithm-based fault tolerance (ABFT). Here we discuss the theory and practice of setting numerical tolerances to separate errors caused by a fault from those inherent in finite-precision numerical calculations.

To separate these two classes of errors, we employ well-known bounds on error-propagation within linear algebraic algorithms. These bounds provide a maximum error that is to be expected due to register effects; any error in excess of this is taken to be the product of a fault. Adapting these bounds to the ABFT setting yields a series of tests having different efficiency and accuracy attributes.

Characteristics of a given scheme are concisely expressed using the standard receiver operating characteristic (ROC) curve. For a given error tolerance,

a certain proportion of False Alarms (numerical errors tagged as data faults) and Detections (data faults correctly identified) will be observed. The ROC plots these two proportions parametrically as the tolerance is varied; this describes the performance achievable by a certain detection scheme and provides a basis for choosing one scheme over others. Two series of tests are described here. The first shows the general effectiveness of the linear ABFT schemes we have proposed, and the second verifies the correct behavior of our parallel implementation of them.

We close this introduction by introducing some useful notation. Matrices and vectors are written in uppercase and lowercase roman letters; A^T is the transpose of the matrix A. Any identity matrix is always I; context provides its dimension. A is *orthogonal* if $AA^\mathsf{T} = I$. A square matrix is a *permutation* if it can be obtained by re-ordering the rows of I. The size of a vector v is measured by its *p-norm*, a non-negative real number $\|v\|_p$; similarly for matrices A. See [3] (hereafter abbreviated GVL), sections 2.2 and 2.3, for the definitions. The *submultiplicative property* of p-norms implies that $\|AB\|_p \leq \|A\|_p \|B\|_p$ and similarly for vectors.

2. General Considerations

In this paper we are concerned with these operations:

- Product: find the product $AB = P$, given A and B.
- LU decomposition: factor A as $A = PLU$ with P a permutation matrix, L unit lower-triangular, and U upper-triangular.
- Singular value decomposition: factor a square A as $A = UDV^\mathsf{T}$, where D is diagonal and U and V are orthogonal matrices.
- System solution: solve for x in $Ax = b$ when given A and b
- Matrix inverse: given A, find B such that $AB = I$.

Although standard linear algebra packages provide many other routines, the ones above were identified by science application teams as the being of the most interest, partly on the basis of amount of time spent within them.

Each of these operations has been written to emphasize that some linear relation holds among the subroutine inputs and its computed outputs; we call this the *postcondition*. For the product, system solution, and inverse, this postcondition is necessary and sufficient, and completely characterizes the subroutine's task. For the other two, the postcondition is only a necessary condition and valid results must enjoy other properties as well. In either case, identifying and checking the postcondition provides a powerful sanity check on the proper functioning of the subroutine.

Before proceeding to examine these operations in detail, we mention two points involved in designing ABFT techniques. Suppose for definiteness that we plan to check one $m \times n$ matrix. Any reasonable checksum scheme must depend on the content of each matrix entry, otherwise some entries would not be checked. This implies that simply computing a checksum requires $O(mn)$ operations. Checksum ABFT schemes thus lose their attractiveness for operations taking $O(mn)$ or fewer operations (e.g. trace, sum, and 1-norm) because it is simpler and more directly informative to achieve fault-tolerance by repeating the computation. The second general point is that, although the postconditions above are linearly-checkable equalities, they need not be. For example, the largest eigenvalue of A is bounded by functions of the 1-norm and the ∞-norm, both of which are easily computed but not linear. One could thus evaluate the sanity of a computation by checking postconditions that involve such inequalities. None of the operations we consider requires this level of generality.

The postconditions we consider generically involve comparing two linear maps, which are known in factorized form

$$L_1 L_2 \cdots L_p \stackrel{?}{=} R_1 R_2 \cdots R_q \quad . \tag{1}$$

This check can be done exhaustively via n linearly independent probes for an $n \times n$ system. Of course, exhaustive comparison would typically introduce about as much computation as would be required to recompute the answer from scratch. On the other hand, a typical fault to data fans out across the matrix outputs, and a single probe would be enough to catch most errors:

$$L_1 L_2 \cdots L_p w \stackrel{?}{=} R_1 R_2 \cdots R_q w \tag{2}$$

for some probe vector w. This is the approach originally recommended by Abraham and his colleagues [4] to implement ABFT in systolic arrays. It has since been extended and refined by several researchers [1, 2, 5, 7].

There are two designer-selectable choices controlling the numerical properties of such an ABFT system: the checksum weights w and the comparison method indicated above by $\stackrel{?}{=}$. When no assumptions may be made about the operands, the first is relatively straightforward: the elements of w should not vary greatly in magnitude so that results figure essentially equally in the check. (In particular, w should be everywhere nonzero.) In what follows, we let w be the vector of all ones; our implementation allows any w to be supplied by the user.

3. Error Propagation: Theory

After the checksum vector, the second choice is the comparison method. As stated above, we perform comparisons using the corresponding postcondition for each operation. To develop a test that is roughly independent of the matrices at hand, we use the well-known bounds on error propagation in linear operations. In what follows, we develop a test for each operation of interest. For each operation, we cite a result bounding the numerical error in the computation's output, and then we use this bound to develop a corollary defining a test which is roughly independent

of the operands. Throughout, we use $\mathbf{u}$ to represent the numerical precision of the underlying hardware; it is the difference between unity and the next larger floating-point number. Also, $\square$ marks the end of a result or corollary.

It is important to understand that the error bounds given in the theorems are *qualitative* and determine the general characteristics of roundoff in our checksum implementations. The estimates we obtain in this section are bounds based on worst-case scenarios, and will typically predict roundoff error larger than practically observed. (See GVL, section 2.4.6, for more on this outlook.) In the ABFT context, using these bounds uncritically would mean setting thresholds too high and missing some fault-induced errors. Their value for us, and it is substantial, is to indicate how roundoff error scales with different inputs. This allows ABFT routines the opportunity to factor out the inputs, yielding performance that is more nearly input-independent. Of course, some problem-specific tuning will likely improve performance. Our goal is to simplify this tuning process as much as possible.

Result 1 *Let* $\hat{P} = \texttt{mult}(A, B)$ *be computed using a dot-product, outer-product, or gaxpy-based algorithm. The* $n \times n$ *forward error matrix* $E = \hat{P} - AB$ *satisfies*

$$\|E\|_\infty \leq n\|A\|_\infty\|B\|_\infty\mathbf{u} \tag{3}$$

Proof. See GVL, section 2.4.8. $\square$

Corollary 2 *An input-independent checksum test for* `mult` *is*

$$d = \hat{P}w - ABw \tag{4}$$

$$\|d\|_\infty/(\|A\|_\infty\|B\|_\infty\|w\|_\infty) \gtrless \tau\mathbf{u} \tag{5}$$

where τ *is an input-independent threshold.*

The test is expressed as a comparison (indicated by the $\gtrless$ relation) with a threshold; the latter is a scaled version of the floating-point accuracy. If the discrepancy is larger than $\tau\mathbf{u}$, a fault would be declared, otherwise the error is explainable by roundoff.

Proof. The difference $d = Ew$ so, by the submultiplicative property of norms and theorem 1,

$$\|d\|_\infty \leq \|E\|_\infty\|w\|_\infty \leq n\|A\|_\infty\|B\|_\infty\|w\|_\infty\mathbf{u}$$

and the dependence on A and B is removed by dividing by their norms. The factor of n is unimportant in this calculation, as noted in the remark beginning the section. $\square$

For the remaining operations, we require the notion of a *numerically realistic* matrix. The reliance of numerical analysts on certain proven algorithms is based on the rarity of certain pathological matrices that cause, for example, pivot elements in decomposition algorithms to grow exponentially. Even algorithms regarded as stable and reliable can be made to misbehave when given such unlikely inputs. Because the underlying routines will fail under such pathological conditions, we may neglect them in designing an ABFT system; such a computation is doomed even without faults. Accordingly, the theorems below must assume that the inputs are numerically realistic to obtain usable error bounds.

Result 3 *Let* $(\hat{P}, \hat{L}, \hat{U}) = \texttt{lu}(A)$ *be computed using a standard* LU *decomposition algorithm with partial pivoting. The backward error matrix* E *defined by* $A + E = \hat{P}\hat{L}\hat{U}$ *satisfies*

$$\|E\|_\infty \leq 8n^3\rho\,\|A\|_\infty\mathbf{u} \tag{6}$$

where the growth factor ρ *depends on the size of certain partial results of the calculation, and is bounded by a small constant for numerically realistic matrices.*

Proof. See GVL, section 3.4.6. $\square$

We note in passing that this is close to the best possible bound for the discrepancy, because the error in simply writing down the matrix A must be of order $\|A\|\mathbf{u}$.

Corollary 4 *An input-independent checksum test for* `lu` *as applied to numerically realistic matrices is*

$$d = \hat{P}\hat{L}\hat{U}w - Aw \tag{7}$$

$$\|d\|_\infty/(\|A\|_\infty\|w\|_\infty) \gtrless \tau\mathbf{u} \tag{8}$$

where τ *is an input-independent threshold.*

Proof. We have $d = Ew$ so, by the submultiplicative property of norms and theorem 3,

$$\|d\|_\infty \leq \|E\|_\infty\|w\|_\infty \leq 8n^3\rho\,\|A\|_\infty\|w\|_\infty\mathbf{u} \quad .$$

As before, the factor of $8n^3$ is unimportant in this calculation. For numerically realistic matrices, the growth factor ρ is bounded by a constant, and the indicated test is recovered by dividing by the norm of A. $\square$

Result 5 *Let* $(\hat{U}, \hat{D}, \hat{V}) = \texttt{svd}(A)$ *be computed using a standard singular value decomposition algorithm. The backward error matrix* E *defined by* $A + E = \hat{U}\hat{D}\hat{V}^\mathsf{T}$ *satisfies*

$$\|E\|_2 \leq \rho\,\|A\|_2\mathbf{u} \tag{9}$$

where ρ *is a constant not much larger than one for numerically realistic matrices* A.

Proof. See GVL, section 5.5.8. $\square$

Corollary 6 *An input-independent checksum test for* `svd` *as applied to numerically realistic matrices is*

$$d = \hat{U}\hat{D}\hat{V}^\mathsf{T}w - Aw \tag{10}$$

$$\|d\|_2/(\|A\|_2\|w\|_2) \gtrless \tau\mathbf{u} \tag{11}$$

where τ *is an input-independent threshold.*

Recommended Checksum Tests

Algorithm	Δ	σ_1	σ_2	σ_3	Note
`mult`	$\hat{P} - AB$	$\|A\|\|B\|$	$\|\hat{P}\|$	$\|\hat{P}w\|$	—
`lu`	$\hat{P}\hat{L}\hat{U} - A$	$\|A\|$	$\|\hat{P}\hat{L}\hat{U}\|$	$\|Aw\|$	σ_1 easier than σ_2
`svd`	$\hat{U}\hat{D}\hat{V} - A$	$\|A\|$	$\|\hat{U}\hat{D}\hat{V}^{\mathsf{T}}\|$	$\|Aw\|$	σ_1 easier than σ_2
`inv`	$I - A\hat{B}$	$\|A\|\|A^{-1}\|$	$\|A\|\|\hat{B}\|$	$\|A\|\|\hat{B}w\|$	$\|A\hat{B}w\|$ useless

Table 1: Algorithms considered here, and recommended checksum tests.

Proof. We have $d = Ew$ so, by the submultiplicative property of norms,

$$\|d\|_2 \leq \|E\|_2\|w\|_2 \leq \rho\,\|A\|_2\|w\|_2\mathbf{u}$$

and the dependence on A is removed by dividing by its norm. The constant ρ is negligible for numerically realistic matrices. □

Corollary 7 *An input-independent checksum test for* `svd` *as applied to numerically realistic matrices is*

$$d = \hat{U}\hat{D}\hat{V}^{\mathsf{T}}w - Aw \tag{12}$$

$$\|d\|_\infty/(\|A\|_\infty\|w\|_\infty) \gtrless \tau\mathbf{u} \tag{13}$$

where τ is an input-independent threshold.

Proof. By corollary 6, the check above with the 2-norm in place of the ∞-norm is an input-independent checksum test. But since these two norms are equivalent in that

$$\|w\|_\infty \leq \|w\|_2 \leq \sqrt{n}\|w\|_\infty$$
$$(1/\sqrt{n})\|A\|_\infty \leq \|A\|_2 \leq \sqrt{m}\|A\|_\infty$$

(see GVL sections 2.2.2 and 2.3.2), the two tests are also equivalent up to negligible constants. □

Result 8 *Let $\hat{B} = \mathtt{inv}(A)$ be computed using Gaussian elimination with partial pivoting. The backward error matrix E defined by $(A+E)^{-1} = \hat{B}$ satisfies*

$$\|E\|_\infty \leq 8n^3\rho\,\|A\|_\infty\mathbf{u} \tag{14}$$

with ρ as in theorem 3.

Proof. See GVL, section 3.4.6, which defines the backwards error for the linear system solution $Ax = b$. Since A^{-1} is calculated by solving the multiple right-hand-side problem $AA^{-1} = I$, the bound given there on $\|E\|_\infty$ applies here with the same growth factor ρ. (This growth factor depends only on the pivots in the LU factorization which underlies the inverse computation.) □

Corollary 9 *An input-independent checksum test for* `inv` *as applied to numerically realistic matrices is*

$$d = w - A\hat{B}w \tag{15}$$

$$\|d\|_\infty/(\|A\|_\infty\|A^{-1}\|_\infty\|w\|_\infty) \gtrless \tau\mathbf{u} \tag{16}$$

where τ is an input-independent threshold.

Proof. See the appendix. □

We remark that this bound on discrepancy, larger than that for `lu`, is the reason matrix inversion is numerically unstable.

4. Error Propagation: Implementation

It is straightforward to transform these results into algorithms for error detection via checksums. The principal issue is computing the desired matrix norms efficiently from results needed in the root calculation. For example, in the matrix multiply, instead of computing $\|A\|\|B\|$, it is more efficient to compute $\|\hat{C}\|$ which equals $\|AB\|$ under fault-free conditions. By the submultiplicative property of norms, $\|AB\| \leq \|A\|\|B\|$, so this substitution always underestimates the upper bound on roundoff error, leading to false alarms. On the other hand, we must remember that the norm bounds are only general guides anyway. All that is needed is for $\|AB\|$ to scale as does $\|A\|\|B\|$; the unknown scale factor can be absorbed into τ.

Taking this one step farther, we might compute $\|\hat{C}w\|$ as a substitute for $\|A\|\|B\|\|w\|$. Here we run an even greater risk of underestimating the bound, especially if w is nearly orthogonal to the product, so it is wise to use instead $\lambda\|w\| + \|\hat{C}w\|$ for some problem-dependent λ. Extending this reasoning to the other operations yields the comparisons in table 1. The error criterion used there always proceeds from the number $\delta = \|\Delta w\|$ for the indicated difference matrix Δ; this matrix is of course never explicitly computed. In addition to the obvious

$$T0: \quad \delta/\|w\| \gtrless \tau\mathbf{u} \quad \text{(trivial test)} \tag{17}$$

we provide three other comparison tests

$$T1: \quad \delta/(\sigma_1\|w\|) \gtrless \tau\mathbf{u} \quad \text{(ideal test)} \tag{18}$$

$$T2: \quad \delta/(\sigma_2\|w\|) \gtrless \tau\mathbf{u} \quad \text{(approximate matrix test)} \tag{19}$$

$$T3: \quad \delta/(\lambda\|w\| + \sigma_3) \gtrless \tau\mathbf{u} \quad \text{(approximate vector test)} \tag{20}$$

The *ideal test* is the one recommended by the theoretical error bounds, and is based on the supplied input

arguments, but may not be computable. In contrast, both approximate tests are based on computed quantities, and may also be suggested by the reasoning above. The *matrix test* involves a matrix norm while the *vector test* involves a vector norm and is therefore more subject to false alarms. (Several variants of the matrix tests are available for these operations.) We note that the obvious vector test for `inv` uses $A\hat{B}w$, but since $\hat{B} = \texttt{inv}(A)$, this test becomes essentially equivalent to the trivial test. We therefore suggest using the vector/matrix test shown in the table.

Clearly the choice of which test to use is based on the interplay of computation time and fault-detection performance for a given population of input matrices. Because of the shortcomings of numerical analysis, we cannot predict definitively that one test will outperform another. The experimental results reported in the next section are one indicator of real performance, and may motivate more detailed analysis of test behavior. Performance in application codes will be another criterion for choosing tests.

5. Results: Simulated Fault Conditions

In this section we show results of Matlab simulations of the proposed checksum tests. These simulations are intended to verify the essential effectiveness of the checksum technique for ABFT, as well as to sketch the relative behaviors of the tests described above. Due to the special nature of the population of test matrices, and the shortcomings of the fault insertion scheme, these results *must not* be taken as anything but an estimate of relative performance, and a rough estimate of ultimate absolute performance.

We briefly describe the simulation setup. In essence a population of random matrices is used as input to a given computation; faults are injected in half these computations, and a checksum test is used to attempt to identify the affected computations. Random test matrices A of a given condition number κ are generated by the rule

$$A = 10^{\alpha} U D_{\kappa} V^{\mathsf{T}} \quad . \tag{21}$$

The random matrices U and V are the orthogonal factors in the QR factorization of two square matrices with normally distributed entries. The diagonal matrix D_{κ} is filled in by choosing random singular values, such that the largest singular value is unity and the smallest is $1/\kappa$. These matrices all have 2-norm equal to unity; the overall scale is set by α which is chosen uniformly at random between -8 and +8. A total of 800 64×64 matrices (forty applications of the rule (21) for each κ in $\{2^1, ..., 2^{20}\}$) is processed.

Faults are injected in half of these runs (400 of 800) by first choosing a matrix to affect, and then flipping exactly one bit of its 64-bit representation. For example, if a call to `mult` is to suffer a simulated fault, first A or B is selected at random, and then one bit of the chosen matrix is toggled. If `lu` is to suffer a fault, one of A, L, or U is selected and the fault is injected. If A was selected, one can expect the computed $\hat{L}$ and $\hat{U}$ to have many incorrect elements; if L was selected, only one element of the LU decomposition would be in error. This scheme is intended to simulate errors occurring at various times within the computation. Within the context of these tests of fault detection ability, we note that forbidding injection of multiple faults makes the detection task harder, because multiple faults would tend to cause larger, more apparent, errors. At the system level, of course, higher fault-injection rates make the computational task harder.

P^* Across Experiments

	Average-Case		Worst-Case	
	All	Sig.	All	Sig.
`mult`	0.86	1.00	0.63	0.92
`inv`	0.78	1.00	0.32	0.50
`lu`	0.60	1.00	0.43	0.90
`svd`	0.78	0.97	0.60	0.87
Mean	0.76	0.99	0.50	0.80

Table 2: Fault detection probability when no false alarms are permitted. Worst-case results are taken from the Matlab gallery matrices. Results when all faults must be detected, and when only significant faults must be detected, are shown.

Next, each of the four tests described above is used to identify faults; for a fixed τ this implies observing a certain false alarm rate and fault-detection rate. The former is the proportion of trials in which a fault did not occur but one was declared (due to an unexpectedly large numerical error); the latter is the proportion in which an injected fault was correctly detected. The pair (P_{fa}, P_d) may be plotted parametrically versus τ to obtain an ROC curve which illustrates the performance achievable by a given test. See figure 1. In these figures, $T0$ and $T3$ are the solid blue lines with dots, with $T0$ in dark blue lying below $T3$. $T2$ is shown in red asterisks, and $T1$, the optimal test, in green crosses.

Of course, some missed fault detections are worse than others since many faults occur in the low-order bits of the mantissa and cause very minor changes in the matrix. Accordingly, a second set of ROCs is shown in figure 2. In this set, faults causing a minute perturbation (less than one part in 10^{-8}, about the accuracy of single-precision floating point) are screened from the results entirely. This curve is more realistic for our applications.

We may make some general observations about the results. Clearly $T0$, the un-normalized test, fares poorly in all experiments. This illustrates the value of the results on error propagation that form the basis for the normalized tests. Generally speaking,

$$T0 \ll T3 < T2 \approx T1 \quad . \tag{22}$$

This confirms theory, in which $T1$ is the ideal test and the others approximate it. In particular, $T1$ and $T2$ are quite similar because generally only an enormous fault can change the norm of a matrix — these cases are easy to detect.

Further, we note that the most relevant part of the ROC curve is when $P_{fa} \approx 0$; we may in fact be interested in the value P^*, defined to be P_d when $P_{fa} = 0$.

Average-case Matrices, All Faults

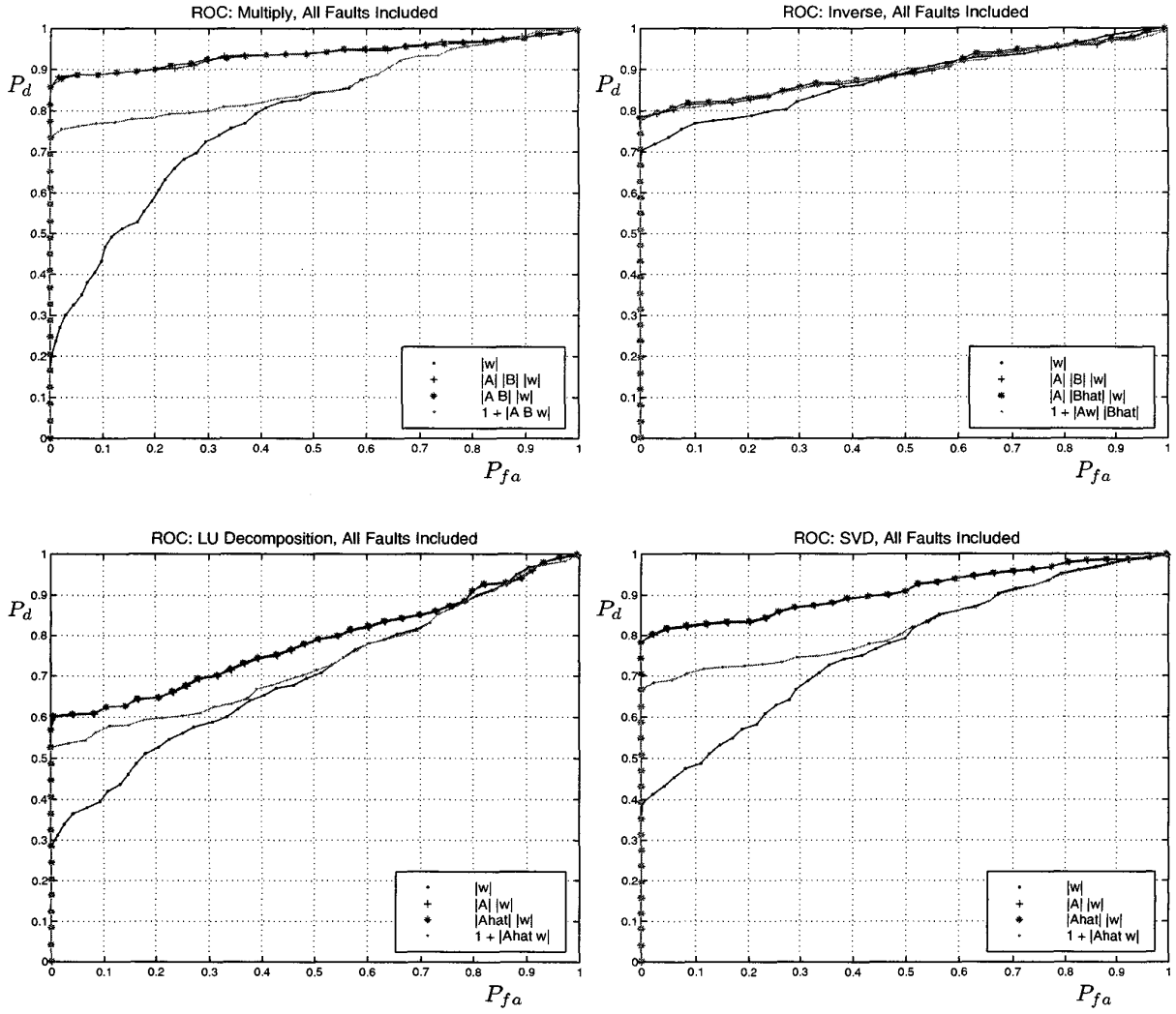

Figure 1: ROC for random matrices of bounded condition number, including all faults.

Average-case Matrices, Significant Faults

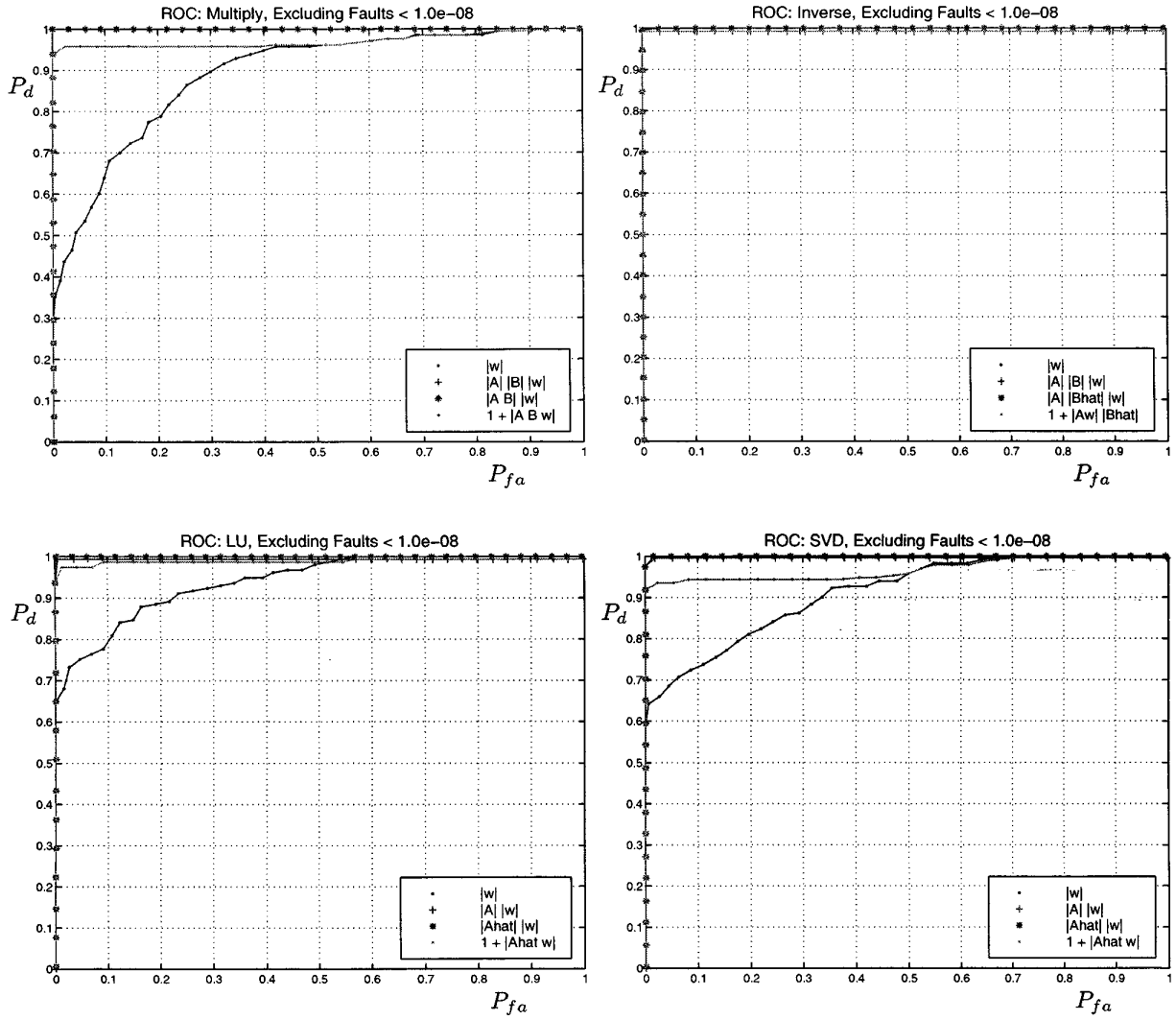

Figure 2: ROC for random matrices of bounded condition number, excluding faults of relative size less than 10^{-8}.

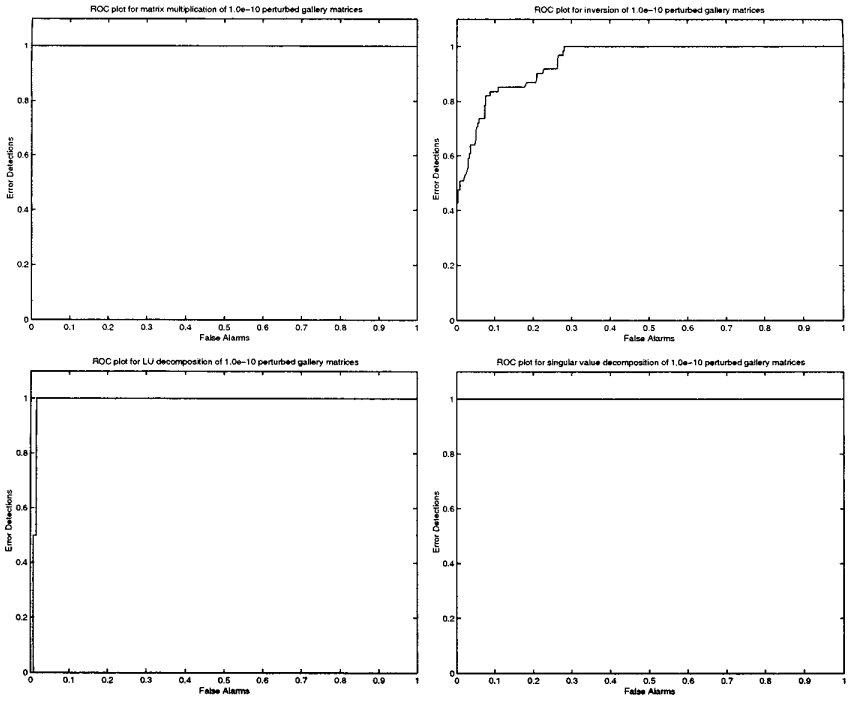

Figure 3: Parallel implementation checked by Matlab computation.

P^* is the detection rate when no false alarms are permitted; it is summarized for these experiments in table 2. The first two columns of this table come from the data in figures 1 and 2; the other columns are from a "worst-case" matrix population taken from the Matlab gallery matrices. Under the average-case test conditions, about 99% of faults could be detected with no false alarms; this level of performance would seem adequate for REE purposes. In worst-case — and no science application should be in this regime — effectiveness drops to about 80%. This quantifies the heuristic idea that fault detection should be more effective for numerically well-posed applications.

6. Results: Fault-free parallel operation

We briefly examine some characteristics of our parallel implementation of the checksum procedures described here. Shown in figure 3 are certain ROC curves for the four operations we have considered. In contrast to the results just reviewed, these curves were generated by checking ScaLAPACK computations with Matlab.[1] ScaLAPACK is a well-known mulitprocessor implementation of many common linear algebraic routines, analogous to LAPACK in the single-processor setting. In this test we use randomly perturbed matrices from the Matlab gallery selection. These matrices are generally ill-conditioned or poorly scaled, but serve as a demanding test set to check our routines against a known standard. In this case, for simplicity, the overall scale parameter $\alpha = 0$ and a fixed perturbation scale $\epsilon = 10^{-10}$ was used.

This time, identical matrix operands are given to Matlab and to our ScaLAPACK implementation. Faults are not injected by modifying operands because our objective is to verify the correct numerical operation of our subroutines. Each system computes the full result matrix; these are combined with the ScaLAPACK checksum comparison to form an ROC as follows. We declare that an error has occurred when the two full results differ by more than a fixed tolerance (10^{-10} in these experiments). An error is declared to have been *detected* or not according to whether a checksum discrepancy was found by the ScaLAPACK implementation. (The Matlab implementation does not compute a checksum; it is used only to find the full result matrix.) With these definitions, a false alarm, for example, means that ScaLAPACK found a checksum discrepancy, but no significant discrepancy was present in the result of the computation. The ROC thus serves as a check, via Matlab, on the numerical characteristics of our ScaLAPACK implementation. In doing these tests, the comparison rule $T0$ was used; this has smaller consequences than in the previous section because most of the perturbed gallery matrices have roughly unit norm.

These curves were generated by sweeping the thresh-

[1] Matlab uses LINPACK `ZGEDI/ZGEFA` for `inv` and `lu`, and `ZSVDC` for `svd`. For `mult`, Matlab uses a straightforward inner product implementation with nested loops. [6]

old τ used in the ScaLAPACK $T0$ test from 0 to ∞. It is clear from the curves that there is excellent agreement between the ScaLAPACK and Matlab versions of `mult`, `lu`, and `svd`. Indeed, when the matrix is badly scaled, ill-conditioned, or numerically unrealistic — causing ScaLAPACK and Matlab to differ according to the full answer — ScaLAPACK finds the error in the checksum calculation also. In essence, the message is: if the computation did not succeed, the checksum test discovers it. Because of the additional instability of the inverse algorithm, its results are less definite. One explanation is that the checksum test is missing some errors that occur in the computed inverse; this needs further investigation.

7. Conclusions

Theoretical results bounding the expected roundoff error in a given computation provide several types of input-independent threshold tests for checksum differences. The observed behavior of these tests is in good general agreement with theory, and readily computable tests are easy to define. All operations considered here (`mult`, `lu` `inv`, and `svd`) admit tests that are effective in detecting faults at the 99% level on typical matrix inputs. Tests of the numerical characteristics of our parallel implementation of the fault detection schemes indicate excellent agreement with another numerical package for most operations, except in cases when the matrix is badly scaled, ill-conditioned, or numerically unrealistic. In those cases, the schemes detect an error in the checksum calculation.

Appendix

Proof of Corollary 9. Note that $d = \Delta w$ where $\Delta = I - A(A+E)^{-1}$. Some algebra is necessary to extract the error E from Δ. Using the Sherman-Morrison formula (GVL section 2.1.3) to rewrite the inverse of $A+E$ we obtain

$$\begin{aligned}\Delta &= I - A[A^{-1} - A^{-1}(I + EA^{-1})^{-1}EA^{-1}] \\ &= (I + EA^{-1})^{-1}EA^{-1} \qquad (23)\end{aligned}$$

For numerically realistic matrices, A dominates E and the first factor is negligible. Heuristically, this is because $E \ll A$ implies $EA^{-1} \ll AA^{-1} = I$, collapsing that factor to I. More formally, inverting a numerically realistic matrix produces an error matrix E such that for any vector v, $\|Ev\| \ll \|Av\|$ otherwise the backward error E would be comparable to A. Since v is arbitrary and A is invertible, we may let $v = A^{-1}u$, obtaining that $\|EA^{-1}u\| \ll \|u\| = \|Iu\|$, showing that the operator EA^{-1} is dominated by I. Therefore we may neglect the first factor and the norm of the error is bounded by

$$\begin{aligned}\|d\|_\infty &= \|\Delta w\|_\infty \\ &\le \|E\|_\infty \|A^{-1}\|_\infty \|w\|_\infty \\ &\le 8n^3\rho \|A\|_\infty \|A^{-1}\|_\infty \|w\|_\infty \mathbf{u} \qquad (24)\end{aligned}$$

using the submultiplicative property of norms. As before, the factor of $8n^3$ is unimportant in this calculation. Invoking the assumption that A is a numerically realistic matrix allows us to neglect the growth factor ρ, yielding the indicated test. □

Acknowledgment

This work was carried out by the Jet Propulsion Laboratory, California Institute of Technology, under contract with the National Aeronautics and Space Administration.

References

[1] D. L. Boley, R. P. Brent, G. H. Golub, and F. T. Luk. Algorithmic fault tolerance using the Lanczos method. *SIAM J. Matrix Anal. Appl.*, 13(1):312–332, 1992.

[2] M. P. Connolly and P. Fitzpatrick. Fault-tolerent QRD recursive least squares. *IEE Proc. Comput. Digit. Tech.*, 143(2):137–144, 1996. IEE, not IEEE.

[3] G. H. Golub and C. F. Van Loan. *Matrix Computations.* Johns Hopkins Univ., Baltimore, second edition, 1989.

[4] K.-H. Huang and J. A. Abraham. Algorithm-based fault tolerance for matrix operations. *IEEE Transactions on Computing*, 33(6):518–528, 1984.

[5] F. T. Luk and H. Park. An analysis of algorithm-based fault tolerance techniques. *Journal of Parallel and Distributed Computing*, 5:172–184, 1988.

[6] MathWorks, 14 April 1999. Personal communication via e-mail from J. Regensburger.

[7] Wang and Jah. Algorithm-based fault tolerance for FFT networks. *IEEE Transactions on Computing*, 43(7):849–854, 1994.

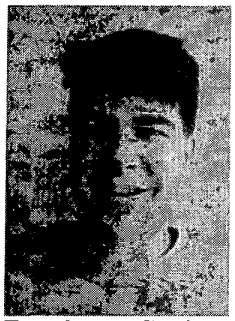

Michael Turmon is a senior member of the technical staff in the Machine Learning Systems Group at the Jet Propulsion Laboratory. He received Bachelor's degrees in Computer Science and in Electrical Engineering from Washington University in St. Louis; he obtained his Ph.D. in Electrical Engineering from Cornell University in 1995. He was a National Science Foundation Graduate Fellow. Michael's areas of research are in the theory of generalization in neural networks, and applications of model-based and nonparametric statistics to scientific image understanding in large databases. He has been theory co-chair on the program committee of the annual NIPS (Neural Information Processing Systems) conference, has been co-investigator on the NASA/ESA SoHO spacecraft, and won the NASA Exceptional Achievement Medal in 1999. He is a member of the IEEE (Information Theory Society) and the Institute for Mathematical Statistics.

Robert Granat is a member of the technical staff in the Machine Learning Systems Group at the Jet Propulsion Laboratory. He received his B.S. in Engineering and Applied Science from the California Institute of Technology, and his M.S. in Electrical Engineering from the University of California, Los Angeles in 1998. Robert's areas of research are in the application of unsupervised learning techniques to large data sets, tomographic imaging, and the modeling of biological vision systems. He is a member of the IEEE.